CLEAN TECHNOLOGY, Vol. 18, No. 4, December 2012, pp. 419~425

청정환경기술

Photocatalysis of Sub-ppm-level Isopropyl Alcohol by Plug-flow Reactor Coated with Nonmetal Elements Irradiated with Visible Light

Wan-Kuen Jo*

Department of Environmental Engineering, Kyungpook National University
1370 Sankeok-dong, Buk-gu, Daegu 702-701, Korea

(Received for review October 24, 2012; Revision received December 7, 2012; Accepted December 7, 2012)

요 약

본 연구는 황 원소와 질소 원소가 도핑된 이산화티타늄의 특성을 조사하고 8-와트(W) 일반 램프와 가시광선 영역의 발광 다이오드 조사 조건에서 낮은 농도수준의 가스상 이소프로필 알코올(isopropyl alcohol, IPA)의 광촉매적 분해능에 대하여 조사하였다. 또한, 이소프로필 알코올의 광촉매 분해시 발생되는 아세톤의 생성에 대해서도 조사하였다. 황 원소와 질소 원소가 도핑된 이산화티타늄의 표면 조사결과, 두 촉매들은 가시광선 조사(visible light-emitting-diodes, LEDs)에 의해 효율적으로 활성화될 수 있는 것으로 나타났다. 두 촉매 모두에 대하여, 공기 유량이 감소함에 따라 이소프로필 알코올의 제거 효율이 증가하는 것으로 나타났다. 황 도핑 촉매의 경우, 유량이 0.1 L min^{-1}일 때 이소프로필 알코올 제거효율이 거의 100%로 나타난 반면에 유량이 2.0 L min^{-1}일 때 이소프로필 알코올 제거효율은 39%로 나타났다. 질소 도핑 촉매의 경우에는, 유량이 0.1 L min^{-1}일 때 이소프로필 알코올 제거효율이 거의 100%로 나타난 반면에 유량이 2.0 L min^{-1}일 때 이소프로필 알코올 제거효율은 90% 이상으로 나타났다. 이소프로필 알코올 제거 효율과는 달리, 유량 감소에 따라 아세톤 생성율은 감소하는 것으로 나타났다. 결과적으로, 아세톤 생성을 최소화하고 이소프로필 알코올 제거 효율을 높이기 위해서는 질소 도핑 촉매를 낮은 유량 조건에서 작동시키는 것이 나은 것으로 나타났다. 또한, 이소프로필 알코올 제거를 위해 가시광선 조사 발광 다이오드보다 8-와트 일반램프가 효율적인 것으로 나타났다.

주제어 : 질소 도핑, 황 도핑, 공기 유량, 아세톤 생성, 발광 다이오드

Abstract : This work explored the characteristics and the photocatalytic activities of S element-doped TiO_2 (S-TiO_2) and N element-doped TiO_2 (N-TiO_2) for the decomposition of gas-phase isopropyl alcohol (IPA) at sub-ppm concentrations, using a plug-flow reactor irradiated by 8-W daylight lamp or visible light-emitting-diodes (LEDs). In addition, the generation yield of acetone during photocatalytic processes for IPA at sub-ppm levels was examined. The surface characteristics of prepared S- and N-TiO_2 photocatalysts were analyzed to indicate that they could be effectively activated by visible-light irradiation. Regarding both types of photocatalysts, the cleaning efficiency of IPA increased as the air flow rate (AFR) was decreased. The average cleaning efficiency determined via the S-TiO_2 system for the AFR of 2.0 L min^{-1} was 39%, whereas it was close to 100% for the AFR of 0.1 L min^{-1}. Regarding the N-TiO_2 system, the average cleaning efficiency for the AFR of 2.0 L min^{-1} was above 90%, whereas it was still close to 100% for the AFR of 0.1 L min^{-1}. In contrast to the cleaning efficiencies of IPA, both types of photocatalysts revealed a decreasing trend in the generation yields of acetone with decreasing the AFR. Consequently, the N-TiO_2 system was preferred for cleaning of sub-ppm IPA to S-TiO_2 system and should be operated under low AFR conditions to minimize the acetone generation. In addition, 8-W daylight lamp exhibited higher cleaning efficiency of IPA than for visible LEDs.

Keywords : N-doped, S-doped, Air flow rate, Acetone generation, Light-emitting-diode

1. Introduction

Heterogeneous photocatalysis over semiconductors has become a promising technology for environmental remediation, since it has a potential to oxidize several organic pollutants and relatively high decomposition efficiency under certain operating conditions [1,2]. In the presence of light illumination over semiconductors, if the energy of the incident light is equivalent to the band gap energy of the semiconductor, electrons would be excited from the valence band to the conduction band of the semiconductor and holes would be left in the valence band[3]. These electrons and holes could undergo subsequent oxidation and reduction reactions with any species, which might be adsorbed on the surface of the semiconductor to give the necessary products. Among several semiconductors, TiO_2 is the most commonly employed photocatalyst due to inexpensive cost, readily availability, and chemical stability[4,5]. However, TiO_2 exhibits a relatively high activity only under UV light, which exceeds the band-gap energy of 3.0 or 3.2 eV in the rutile or anatase crystalline phase, respectively, limiting its practical applications[6].

As such, modification of photocatalysts for the enhancement

* To whom correspondence should be addressed.
E-mail: wkjo@knu.ac.kr

doi:10.7464/ksct.2012.18.4.419

of light absorption and photocatalytic activity under visible light irradiation has been the focus of recent studies.

In particular, TiO_2 photocatalysts impregnated with non-metal elements, such as sulfur (S) and nitrogen (N), have received more recent attention as one of the most attractive photocatalyst groups that exhibit relatively high activities under visible light [7-10]. It is noteworthy that calcination temperature of a photocatalyst for a preparation process can be an important factor, which influences its surface characteristics and thus, its photocatalytic activities[11,12]. As compared with unmodified TiO_2, this kind of study was much less reported for element-doped photocatalysts in literature. This assertion has led the present study to investigate the effects of calcinations temperatures of the element-doped photocatalysts on surface characteristics and photocatalytic activities for environmental applications.

The current study investigated the characteristics and the photocatalytic activities of S element-doped TiO_2 (S-TiO_2) and N element-doped TiO_2 (N-TiO_2) for the decomposition of gas-phase isopropyl alcohol (IPA) also called 2-propanol at sub-ppm concentrations, which are associated with indoor air quality rather than industrial emission levels. This was accomplished using a plug-flow reactor coated with the as-prepared element-doped photocatalysts. Moreover, this study examined the applicability of light-emitting-diodes (LEDs) for the photocatalytic processes as a light source, because they have newly received attention for photocatalytic applications, since they are more efficient in converting electricity into light due to high quantum yields close to unity, thereby leading to low electricity consumption[13]. The target compounds, IPA is generally detected at higher concentration levels in indoor than outdoor environments[14]. In addition, this compound is a prototype VOC (volatile organic compound) for photocatalytic studies because the initial reaction pathway involves almost exclusively the partial oxidation to acetone[15]. Therefore, this study also investigated the generation yield of acetone during photocatalytic processes for IPA at sub-ppm levels. It is highlighted that this study has a unique characteristic in that the element-doped photocatalysts combined with LED as a light source were applied for the photocatalytic decomposition of low-level gas-phase species.

2. Methods

2.1. Preparation and characterization of visible-light-activated photocatalysts

Two types of visible-light-activated photocatalysts (S- and N-TiO_2) were prepared. For S-TiO_2 powders, titanium isopropoxide (TIP, 100.0 g) was mixed with thiourea (107.2 g) at a molar ratio of 1 : 4 in ethanol (1,000 mL). The mixture was stirred at room temperature for 1 h, and a white slurry was obtained after the evaporation of ethanol. A white powder was obtained after leaving the white slurry for 3 days at room temperature. This white powder was calcined at 450 ℃ for 1 h under aerated conditions.

Urea was used as an N source to prepare N-TiO_2 photocatalysts. Eight gram of Degussa P25 TiO_2 powder was added to 20 mL of aqueous solution of urea and stirred at room temperature for 1 h. The resulting mixture was left in the dark for 1 day and then dried under reduced pressure. N-doped TiO_2 powder was calcined at 450 ℃ for 1 h under aerated conditions to obtain yellow powder. The calcined powder was washed with diluted sulfuric acid and then with pure water, and vacuum-dried.

The prepared S- and N-TiO_2 powders, along with the reference pure TiO_2, were characterized using an X-ray diffraction (XRD) meter, a diffuse reflectance ultraviolet-visible-near infrared (UV-VIS-NIR) spectrophotometer, and a Fourier-Transform Infrared (FTIR) spectrometer. XRD patterns were determined on a Rigaku D/max-2500 diffractometer with Cu K_α radiation operated at 40 kV and 100 mA. Visible absorption spectra were obtained for the dry pressed disk samples using a Varian CARY 5G spectrophotometer equipped with an integrating sphere. FTIR analysis was performed on a PerkinElmer Spectrum GX spectrophotometer at a resolution of 4 cm^{-1} in the spectral range of 400-4,000 cm^{-1}.

2.2. Survey protocol

A plug-flow type photocatalytic reactor was constructed using two Pyrex tubes with different diameters but with a same length (26.5 cm) (Figure 1). A conventional lamp or a hexahedral tube installed with visible LED lamps was inserted inside the smaller-diameter Pyrex tube. The inner wall of the outer Pyrex tube was coated with a thin film of the N- or S-TiO_2 photocatalyst. The reactor was designed to direct the flow of incoming air toward the UV light in order to increase the air turbulence inside the reactor, thereby enhancing the distribution of the target compounds onto the photocatalyst surface. The standard gas (0.1 ppm) was prepared by injecting standard IPA into a mixing chamber via a syringe pump (Model 210, KdScientific Inc.).

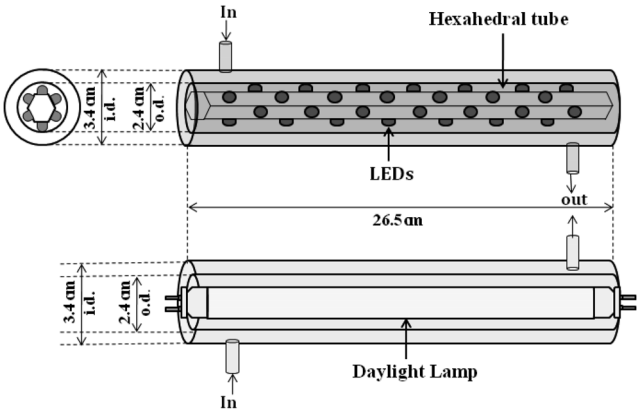

Figure 1. Schematic diagram of photocatalytic reactor.

The prepared gas was flowed through the annular region between the two Pyrex tubes. Its humidity level was adjusted by passing zero-grade air through a charcoal filter, followed by a humidification device in a water bath. The air flow rate (AFR) was controlled using rotameters calibrated against a dry test meter.

The photocatalytic activities of N- and S-TiO_2 powders were evaluated at specified operational conditions. Major operational parameters involved the AFRs and type of light sources. The AFR range for these experiments was 0.1-2.0 L min^{-1} (0.1, 0.5, 1.0, and 2.0 L min^{-1}) to cover a broad range. In addition, two different light sources (conventional 8-W daylight fluorescent lamp and visible LEDs) were used to test their effects on the photocatalytic degradation for IPA. Other parameters were fixed to their representative values: light source, visible LEDs; initial concentration, 0.1 ppm; relative humidity, 50-55%; and AFR, 0.5 L min^{-1}.

For the evaluation of the photocatalytic control efficiencies of IPA and the generation yield of acetone, a time series of gaseous measurements were collected at the inlet and outlet of the photocatalytic reactor prior to and after turning on the lamp. Prior to turning on the lamp, six 10-min samples were collected at 1 h interval for 3 h. Three hours after the introduction of the target compounds (after adsorption equilibrium), the lamp was turned on, and another series of six 10-min samples were collected at 1 h interval for 3 h. The catalyst was pretreated for several hours by making zero-grade air flow through the illuminated reactor. The catalyst pretreatment was performed after the humidity level at the reactor outlet reached equilibrium. When no contamination with the target compounds was measured in the reactor, the target compounds were introduced. The photocatalytic tests were performed under visible-light irradiation conditions, whereas the adsorption tests were done in the absence of visible-light irradiation.

Gas samples were collected by filling an evacuated 5-L Tedlar bag at a constant flow rate. Air from this bag was then drawn through a sorbent trap containing 0.3 grams of Tenax TA using a constant flow-sampling pump (A.P. Buck Inc. Model I.H). All samples were taken at ambient room temperature. The target compounds collected on the sorbent trap were analyzed by coupling a thermal desorption system (SPIS TD, Donam Inc.) to a gas chromatograph (Agilent 7890A) with a flame ionization detector using a 0.32-mm-i.d. by 60-m-length fused silica column (SPB-5, Supelco Co.). The quality assurance/quality control program for the measurement of target compounds included laboratory blank traps and spiked samples.

3. Results and Discussion

3.1. Surface characteristics of photocatalysts

The particle morphologies of S- and N-TiO_2, along with the reference pure TiO_2, were observed by utilizing XRD patterns, UV-vis spectroscopy, and FTIR patterns. Figure 2 illustrates the XRD patterns of pure TiO_2 and S- and N-TiO_2. For all types of photocatalysts, a major peak was appeared at (2θ = 25.2°), which is assigned to anatase crystal phase[12,16]. However, S-TiO_2 and pure TiO_2 showed a peak at 2θ = 27.4°, which is attributed to rutile crystal phase, whereas N-TiO_2 did not. These results are ascribed to the difference of Ti source for the preparation of S- and N-TiO_2 photocatalysts. The S-TiO_2 photocatalysts was prepared using TIP as a Ti source, while N-TiO_2 was prepared using the Degussa P25 TiO_2. Therefore, the XRD patterns were similar for pure TiO_2 and N-TiO_2 photocatalyst. In addition, it is noteworthy that the locations for major XRD peaks were nearly same for the two types of photocatalysts (pure TiO_2 and N-TiO_2), although their intensities were not. This is likely due to the low amounts of nitrogen in the N-TiO_2 photocatalysts, respectively.

Figure 3 exhibits the UV-Vis absorbance spectra of S- and

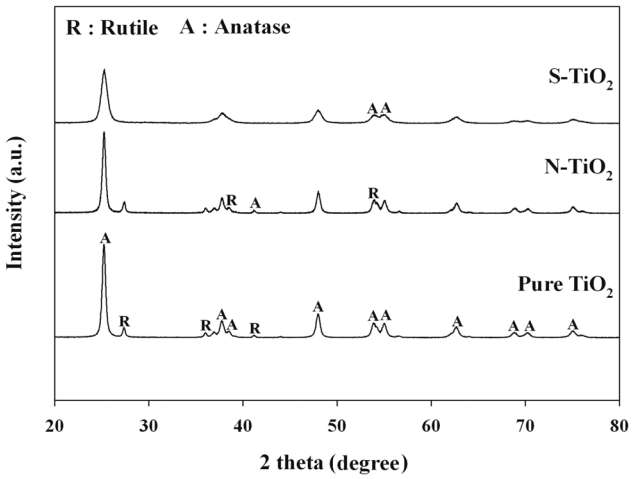

Figure 2. XRD pattern of photocatalysts (S-TiO_2, N-TiO_2, and unmodified TiO_2).

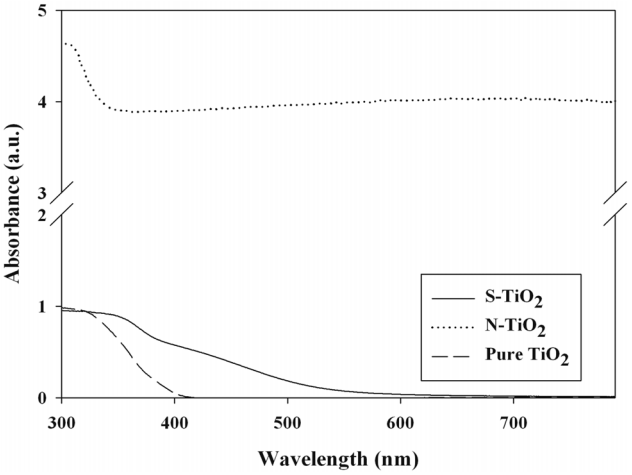

Figure 3. UV-visible spectra of photocatalysts (S-TiO_2, N-TiO_2, and unmodified TiO_2).

N-TiO_2, along with pure TiO_2. Pure TiO_2 photocatalysts presented the absorption edge at $\lambda \approx 400$ nm, which were consistent with the results obtained other studies[16-18]. However, for both S- and N-TiO_2 photocatalysts, the light absorption region was red-shifted. This light absorption shift for S- and N-TiO_2 was also reported by other studies [7,8,17,19]. The shifted absorption edges for the S- and N-TiO_2 photocatalysts were attributed to S and N element doped into TiO_2 particles, respectively[7,17, 19,20]. Consequently, it was identified that in the doping techniques used in the present work, S or N atoms were incorporated into two different sites of the bulk phase of TiO_2. In turn, these findings suggested that the prepared S- and N-TiO_2 photocatalysts could be effectively activated by visible-light irradiation. Meanwhile, a higher N-TiO_2 absorbance level was obtained in all visible regions, in comparison to the S-TiO_2 result. However, it is noteworthy that this pattern may be reversed, depending on the synthesis routes of the two types of photocatalysts.

The FTIR spectra of pure TiO_2 and S- and N-TiO_2 are presented in Figure 4. The absorption peaks of all types of photocatalysts were very similar among another, although their intensities are somewhat different. The major absorption peaks were observed at 3,411, 1,630, and < 1,000 cm^{-1}. The peak at 3,411 cm^{-1} would correspond to the hydroxyl (O-H) stretching vibration, while the band at 1,630 cm^{-1} was ascribed to O-H bending of adsorbed water molecules[19,21,22]. When compared with that of pure TiO_2 previously reported by other researchers as well [23,24], the frequency was moved to a slightly lower wavelength for both types of the N- and S-TiO_2. This frequency movement is likely due to the interaction between the doped N or S and H atoms[24,25]. The bands below 1,000 cm^{-1} are assigned to the titania crystal lattice vibration[21,22]. It is noteworthy that no distinct N- or S-associated peaks were observed for the FTIR results of the as-prepared photocatalysts. This is attributable to small amounts of N or S elements doped into TiO_2[19,21,22].

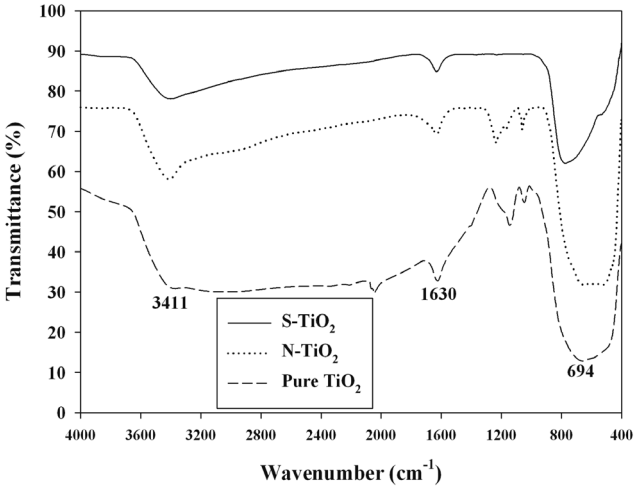

Figure 4. FTIR spectra of photocatalysts (S-TiO_2, N-TiO_2, and unmodified TiO_2).

3.2. Cleaning efficiencies of IPA and generation yield of acetone via S- and N-TiO_2 systems

The cleaning efficiencies for IPA determined via N- and S-TiO_2 photocatalysts were determined in the presence of visible-light. Figures 5(a) and 6(a) exhibit the photocatalytic degradation efficiencies of IPA obtained from the photocatalytic units with S- and N-TiO_2 photocatalysts, respectively, according to AFR. Regarding both types of photocatalysts, the cleaning efficiency of IPA increased as the AFR was decreased. The average cleaning efficiency determined via the S-TiO_2 system for the AFR of 2.0 L min^{-1} was 39%, whereas it was close to 100% for the AFR of 0.1 L min^{-1}. Regarding the N-TiO_2 system, the average cleaning efficiency for the AFR of 2.0 L min^{-1} was above 90%, whereas it was still close to 100% for the AFR of 0.1 L min^{-1}. As such, under the experimental conditions used in this study, the N-TiO_2 system revealed superior performance for cleaning of IPA to S-TiO_2 system. Moreover, as AFR was increased, the

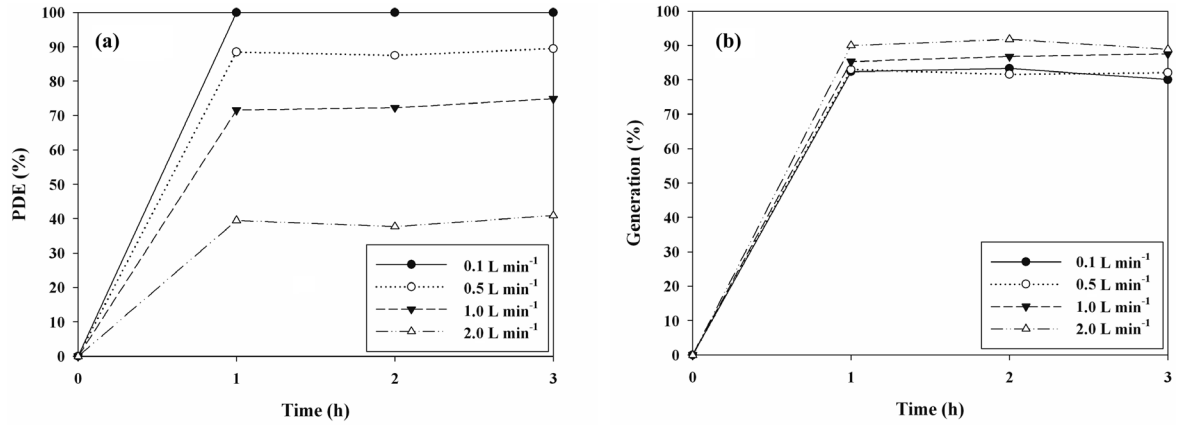

Figure 5. Photocatalytic decomposition efficiency of isopropyl alcohol (a) and generation yield of acetone (b) as determined via photocatalytic systems with S-TiO_2, according to flow rate (0.1, 0.5, 1.0, and 2.0 L min^{-1}).

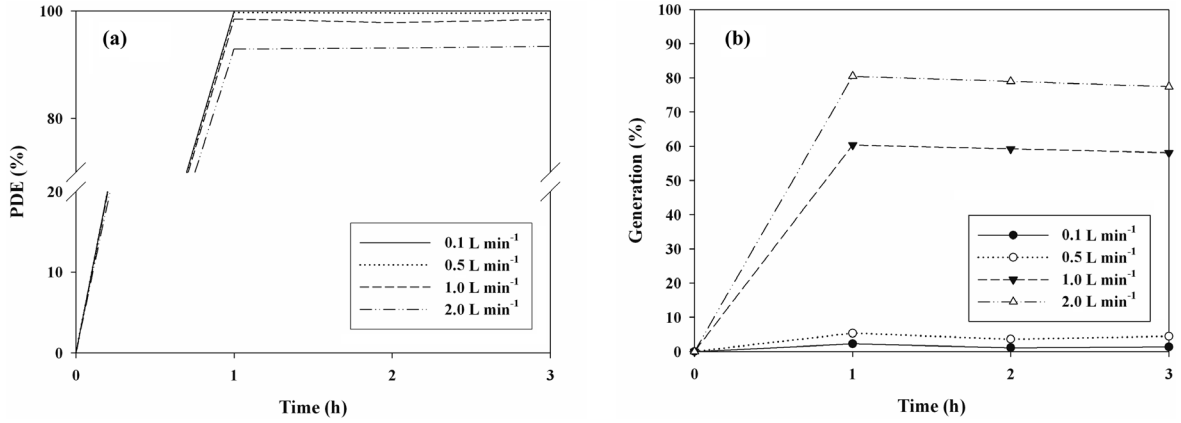

Figure 6. Photocatalytic decomposition efficiency of isopropyl alcohol (a) and generation yield of acetone (b) as determined via photocatalytic systems with N-TiO_2, according to flow rate (0.1, 0.5, 1.0, and 2 L min^{-1}).

bulk mass transport of target compounds from the gas-phase to the surface of the catalyst particle, which is an important heterogeneous catalytic reaction process, would be increased mainly due to convection and diffusion[26]. As such, the decomposition rate would increase as AFR was increased, indicating that IPA decomposition is limited to mass transfer to the surface of photocatalysts. However, this pattern is a contrast to that determined in the current study. At higher AFRs the gas retention time in the photocatalytic reactor would be too short to provide sufficient IPA transfer from the gas phase to the solid catalyst surface [26,27]. The gas retention times in the current study were 72, 14.4, 7.2, and 3.6 s for AFRs of 0.1, 0.5, 1.0, and 2.0 L min^{-1}, respectively. They were determined by dividing the photocatalytic reactor volume by AFR. Consequently, the lower efficiencies at higher AFRs indicated that an insufficient reactor retention time effect would exceed the bulk mass transport effect on IPA decomposition on the catalyst surfaces.

Figures 5(b) and 6(b) shows the generation yields of acetone determined via S- and N-TiO_2 photocatalytic systems, respectively, according to AFR. This acetone generation is ascribed to the partial oxidation of IPA[15,28,29]. In contrast to the cleaning efficiencies of IPA, both types of photocatalysts revealed a decreasing trend in the generation yields of acetone with decreasing the AFR. The average generation yield of acetone obtained from the S-TiO_2 system for the AFR of 2.0 L min^{-1} was 90%, whereas it was 80% for the AFR of 0.1 L min^{-1}. As regards the N-TiO_2 system, the average generation yield of acetone for the AFR of 2.0 L min^{-1} was above 79%, whereas it was still close to zero for the AFR of 0.1 L min^{-1}. The N-TiO_2 system, which exhibited higher cleaning efficiency of IPA, showed lower generation yield of acetone. Consequently, these findings indicate that the N-TiO_2 system is preferred for cleaning of sub-ppm IPA to S-TiO_2 system and should be operated under low AFR conditions to minimize the acetone generation.

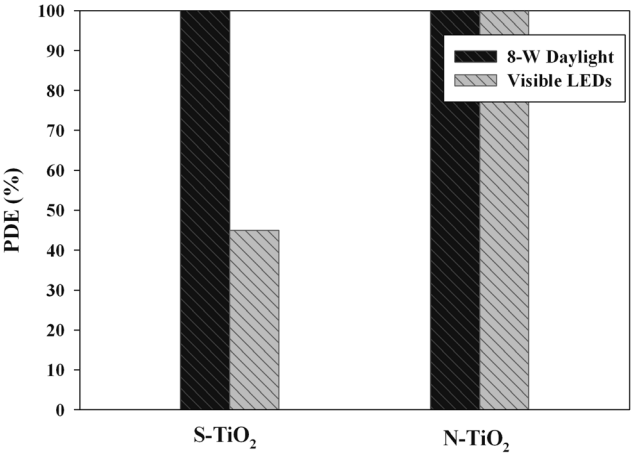

Figure 7. Photocatalytic decomposition efficiency of isopropyl alcohol as determined via photocatalytic systems with S-TiO_2 and N-TiO_2, respectively, according to light source type: conventional 8-W daylight fluorescent lamp and visible LEDs.

Figure 7 allows the comparison of two light sources (8-W daylight and visible LEDs) for their IPA cleaning efficiencies determined via S- and N-TiO_2 photocatalysts. For S-TiO_2 system, the cleaning efficiency of IPA was much higher for the 8-W daylight lamp than for the LEDs. However, the effect of light source type on cleaning efficiency of IPA was indistinguishable because both light sources exhibited cleaning efficiencies of close to 100% for the N-TiO_2 system. Photocatalytic degradation efficiency is proportional to light intensity[30,31]. However, the daylight (1.1 mW cm^{-2}), which exhibited higher IPA cleaning efficiency, had lower light intensity compared to that of the LEDs (2.2 mW cm^{-2}). These findings suggest that under the experimental conditions used in this study, light intensity was not an influential parameter for the difference in degradation efficiency between daylight lamp and LEDs. Rather, the wavelength of daylight lamp was distributed at a wide range of 400-

720 nm, which comprised low wavelengths compared to that of the LEDs (470 nm). Thus, the higher cleaning efficiency for the daylight lamp system was most likely due to its higher light energy at a low wavelength. In addition, the N-TiO_2/LED system showed higher decomposition efficiency of IPA than that of S-TiO_2/LED system. These findings are ascribed to the greater specific surface area of the N-TiO_2 (43.2 m^2 g^{-1}) compared to S-TiO_2 (28.3 m^2 g^{-1}).

4. Conclusions

This study explored the cleaning efficiency of IPA and generation yield of acetone using S- and N-TiO_2 photocatalytic systems under visible-light irradiation. According to the survey of surface characteristics of prepared S- and N-TiO_2 photocatalysts, it was indicated that they could be effectively activated by visible-light irradiation. Regarding both types of photocatalysts, the cleaning efficiency of IPA increased as the AFR was decreased, likely due to insufficient reactor retention time at higher AFRs. The N-TiO_2 system was preferred for cleaning of sub-ppm IPA to S-TiO_2 system and should be operated under low AFR conditions to minimize the acetone generation. Moreover, 8-W daylight lamp exhibited higher cleaning efficiency of IPA than for visible LEDs, likely due to its higher light energy at a low wavelength, but not light intensity.

Acknowledgements

This work was supported by the National Research Foundation of Korea (NRF) grant funded by the Korea government (MEST) (No. 2011-0027916).

References

1. Bouzaza, A., Vallet, C., and Laplanche, A., "Photocatalytic Degradation of Some VOCs in the Gas Phase Using an Annular Flow Reactor: Determination of the Contribution of Mass Transfer and Chemical Reaction Steps in the Photodegradation Process," *J. Photochem. Photobiol. A*, **177**, 212-217 (2007).
2. Sekiguchi, K., Morinaga, W., Sakamoto, K., Tamura, H., Yasui, F., Mehrjouei, M., Müller, S., and Möller, D., "Degradation of VOC Gases in Liquid Phase by Photocatalysis at the Bubble Interface," *Appl. Catal.*, **97**, 190-197 (2010).
3. Herrmann, J. M., "Fundamentals and Misconceptions in Photocatalysis," *J. Photochem. Photobiol. A*, **216**, 85-93 (2010).
4. Han, F., Kambala, V. S. R., Srinivasan, M., Rajarathnam, D., and Naidu, R., "Tailored Titanium Dioxide Photocatalysts for the Degradation of Organic Dyes in Wastewater Treatment: A Review," *Appl. Catal. A*, **359**, 25-40 (2009).
5. Paz, Y., "Application of TiO_2 Photocatalysis for Air Treatment: Patents' Overview," *Appl. Catal. B*, **99**, 448-460 (2010).
6. Chatterjee, D., and Dasgupta, S., "Visible Light Induced Photocatalytic Degradation of Organic Pollutants," *J. Photochem. Photobiol. C*, **6**, 186-205 (2005).
7. Yamada, K., Yamane, H., Matsushima, S., Nakamura, H., Ohira, K., Kouya, M., and Kumada, K., "Effect of Thermal Treatment on Photocatalytic Activity of N-doped TiO_2 Particles under Visible Light," *Thin Solid Films*, **516**, 7482-7487 (2008).
8. Bayati, M. R., Moshfegh, A. Z., and Golestani-Fard, F., "On the Photocatalytic Activity of the Sulfur Doped Titania Nanoporous Films Derived via Micro-arc Oxidation," *Appl. Catal. A*, **389**, 60-67 (2010).
9. Jo, W. K., and Yang, C. H., "Visible-light-induced Photocatalysis of Low-level Methyl-tertiary Butyl Ether (MTBE) and Trichloroethylene (TCE) Using Element-doped Titanium Dioxide," *Build. Environ.*, **45**, 819-824 (2010).
10. Sun, H., Wang, S., Ang, H. M., Tade, M. O., and Li, Q., "Halogen Element Modified Titanium Dioxide for Visible Light Photocatalysis," *Chem. Eng. J.*, **162**, 437-447 (2010).
11. Mahdjoub, N., Allen, N., Kelly, P., and Vishnyakov, V., "SEM and Raman Study of Thermally Treated TiO_2 Anatase Nanopowders: Influence of Calcination on Photocatalytic Activity," *J. Photochem. Photobiol. A*, **211**, 59-64 (2010).
12. Luís, A. M., Neves, M. C., Mendonça, M. H., and Monteiro, O. C., "Influence of Calcination Parameters on the TiO_2 Photocatalytic Properties," *Mater. Chem. Phys.*, **125**, 20-25 (2011).
13. http://en.wikipedia.org/wiki/Light-emitting_diode
14. Jia, C., Batterman, S., and Godwin, C., "VOCs in Industrial, Urban and Suburban Neighborhoods-Part 2: Factors Affecting Indoor and Outdoor Concentrations," *Atmos. Environ.*, **42**, 2101-2116 (2008).
15. Vildozo, D., Ferronato, C., Sleiman, M., and Chovelon, J. -M., "Photocatalytic Treatment of Indoor Air: Optimization of 2-propanol Removal Using a Response Surface Methodology (RSM)," *Appl. Catal. B*, **94**, 303-310 (2010).
16. Jo, W. K., and Kim, J. T., "Application of Visible-light Photocatalysis with Nitrogen-doped or Unmodified Titanium Dioxide for Control of Indoor-level Volatile Organic Compounds," *J. Hazard. Mater.*, **164**, 360-366 (2009).
17. Horikawa, T., Katoh, M., and Tomida, T., "Preparation and Characterization of Nitrogen-doped Mesoporous Titania with High Specific Surface Area," *Microp. Mesop. Mater.*, **110**, 397-404 (2008).
18. Qin, X., Jing, L., Tian, G., Qu, Y., and Feng, Y., "Enhanced Photocatalytic Activity for Degrading Rhodamine B Solution of Commercial Degussa P25 TiO_2 and its Mechanisms," *J. Hazard. Mater.*, **172**, 1168-1174 (2009).
19. Nam, S. H., Kim, T. K., and Boo, J. H., "Physical Property and Photo-catalytic Activity of Sulfur Doped TiO_2 Catalysts Responding to Visible Light," *Catal. Today*, **185**, 259-262

(2012).

20. Ohno, T., Akiyoshi, M., Umebayashi, T., Asai, K., Mitsui, T., and Matsumura M, "Preparation of S-doped TiO_2 Photocatalysts and their Photocatalytic Activities under Visible Light," *Appl. Catal. A*, **265**, 115-121 (2004).
21. Soler-Illia, G. J. A. A., Louis, A., and Sanchez, C., "Sybthesis and Characterization of Mesostructured Titania-based Materials through Evaporation-induced Self-assembly," *Chem. Mater.*, **14**, 750-759 (2002).
22. Peng, T., Zhao, D., Dai, K., Shi, W., and Hirao, K., "Synthesis of Titanium Dioxide Nanoparticles with Mesoporous Anatase Wall and High Photocatalytic Activity," *J. Phys. Chem. B*, **109**, 4947-4952 (2005).
23. Augugliaro, V., Kisch, H., Loddo, V., López-Muñoz, M. J., Márquez-Álvarez, C., Palmisano, G., Palmisano, L., Parrino, F., and Yurdakal, S., "Photocatalytic Oxidation of Aromatic Alcohols to Aldehydes in Aqueous Suspension of Home Prepared Titanium Dioxide 2. Intrinsic and Surface Features of Catalysts," *Appl. Catal. A*, **349**, 189-197 (2008).
24. Nolan, N. T., Synnott, D. W., Seery, M. K., Hinder, S. J., Wassenhoven, A. V., and Pillai, S. C., "Effect of N-doping on the Photocatalytic Activity of Sol-gel TiO_2," *J. Hazard. Mater.*, **211-212**, 88-94 (2012).
25. Madarász, J., Brăileanu, A., Crişan, M., and Pokol, G., "Comprehensive Evolved Gas Analysis (EGA) of Amorphous Precursors for S-doped Titania by in situ TG-FTIR and TG/DTA-MS in Air: Part 2. Precursor from Thiourea and Titanium(IV)-n-butoxide," *J. Anal. Appl. Pyrol.*, **85**, 549-556 (2009).
26. Boulinguiez, B., Bouzaza, A., Merabet, S., and Wolbert, D., "Photocatalytic Degradation of Ammonia and Butyric Acid in Plug-flow Reactor: Degradation Kinetic Modeling with Contribution of Mass Transfer," *J. Photochem. Photobiol. A*, **200**, 254-261 (2008).
27. Li, D., Xiong, K., Yang, Z., Liu, C., Feng, X., and Lu, X., "Process Intensification of Heterogeneous Photocatalysis with Static Mixer: Enhanced Mass Transfer of Reactive Species," *Catal. Today*, **175**, 322-327 (2011).
28. Arsac, F., Bianchi, D., Chovelon, J. M., Ferronato, C., and Herrmann, J. M., "Experimental Microkinetic Approach of the Photocatalytic Oxidation of Isopropyl Alcohol on TiO_2. Part 1. Surface Elementary Steps Involving Gaseous and Adsorbed C_3 H_xO Species," *J. Phys. Chem. B*, **110**, 4202-4212 (2006).
29. Den, W., and Wang, C. C., "Enhancement of Adsorptive Chemical Filters via Titania Photocatalysts to Remove Vapor-phase Toluene and Isopropanol," *Sep. Purif. Technol.*, **85**, 101-111 (2012).
30. Demeestere K., Dewulf J., and Van Langenhove H., "Heterogeneous Photocatalysis as an Advanced Oxidation Process for the Abatement of Chlorinated, Monocyclic Aromatic and Sulfurous Volatile Organic Compounds in Air: State of the Art," *Crit. Rev. Environ. Sci. Technol.*, **37**, 489-538 (2007).
31. Liu B., and Zhao X., "A Kinetic Model for Evaluating the Dependence of the Quantum Yield of Nano-TiO_2 Based Photocatalysis on Light Irradiance, Grain Size, Carrier Lifetime, and Minority Carrier Diffusion Coefficient: Indirect Interfacial Charge Transfer," *Electrochimica Acta*, **55**, 4062-4070 (2010).